Homolytic C−S Bond Scission in the Desulfurization of Aromatic and Aliphatic Thiols Mediated by a Mo/Co/S Cluster: Mechanistic Aspects Relevant to HDS Catalysis

M. David Curtis* and Scott H. Druker

Contribution from the Willard H. Dow Laboratory, Department of Chemistry, The University of Michigan, Ann Arbor, Michigan 48109-1055

Received June 24, 1996[⊗]

Abstract: The kinetics of the reaction of a series of aromatic and aliphatic thiols with cluster **1** were determined. These reactions form cluster **2** and the arene or alkane corresponding to the thiol: $Cp'_2Mo_2Co_2S_3(CO)_4$ (**1**) + RSH → $Cp'_2Mo_2Co_2S_4(CO)_2$ (**2**) + RH + 2CO. These reactions are first order in thiol and first order in cluster **1** with appreciable negative entropies of activation. These data suggest that the rate determining step of the desulfurization reaction is the initial association of the thiol to the cluster. The more nucleophilic thiolate anions react with **1** at −40 °C to form an adduct in which the thiolate anion is bound η^1 to the Co atom. At −25 °C, the initial adduct rearranges to a fluxional μ_2, η^1-bound thiolate. The fluxional process is proposed to involve a concerted "walking" of the thiolate and a μ_2-bound sulfide ligand on the surface of the cluster. Near 35 °C, the thiolate−cluster adduct undergoes C−S bond homolysis to give the paramagnetic anion of cluster **1** and the phenyl or alkyl radical. The radical nature of the C−S bond cleavage was confirmed by the desulfurization of the radical clock reagents, cyclopropylmethanethiol and -thiolate anion, that form the cyclopropylmethyl radical which rearranged to the butenyl radical. The possible similarity in the C−S bond cleavage mechanism in these desulfurization reactions to those occurring in hydrodesulfurization (HDS) over Co/Mo/S catalysts is discussed.

Introduction

Hydrodesulfurization (HDS) is a catalytic process used world wide to remove sulfur from fossil fuels. The presence of sulfur acts as a poison to the precious metal catalysts used in refining reactions, e.g. catalytic reforming and catalytic cracking, and the SO_x formed during combustion of the fuel is an undesirable environmental pollutant.[1] Nearly all hydrotreating catalysts are composed of a group 6 element (Mo or W) associated with a "promoter" element (Co or Ni) deposited on a support, typically Al_2O_3.[1,2] One of the most commonly used HDS catalyst is composed of a mixture of Mo and Co sulfides supported on Al_2O_3. Over the past 15 years, a great deal of research has focused on identifying the architecture of the HDS catalyst in order to better understand how the catalyst works.[1,2] Based on extensive physical characterization by EXAFS, emission Mössbauer spectroscopy, IR, X-ray diffraction, and electron microscopy, the model that currently is most accepted is the "CoMoS" phase model of Topsøe's group.[1a] In this model of the catalyst active site, the Co atoms decorate the edges of MoS_2 crystallites that are on the surface of the support. However, this physical model is not easily related to the mechanism by which C−S bonds are cleaved nor to the chemical role played by the Co promoter element.

Organometallic models are especially useful in the case of complex catalysts, e.g. the HDS catalyst. Organometallic compounds can provide well-defined structural models whose spectral properties may be used to interpret the spectra of the complex catalyst. Similarly, the types of reactions exhibited by organometallic compounds in solution are often found to occur also on the surface of heterogeneous catalysts, and the mechanistic understanding obtained in solution can often be applied to the surface counterparts. We have been modeling the HDS catalyst with Mo/Co/S clusters, e.g. **1** and **2**, and have shown that a variety of organic sulfides are desulfurized by **1** with the concomitant formation of cluster **2** (Scheme 1).[3−5] The lack of skeletal rearrangements or olefin formation and the stereoselectivity of the desulfurization of thiiranes suggested that the mechanism of the desulfurization reaction does not involve the generation of carbocations. Furthermore, the facile desulfurization of isothiocyanates with a C═S double bond, and the fact that desulfurizations of aromatic and aliphatic thiols qualitatively occur at comparable rates in spite of different C−S bond energies, suggested that C−S bond cleavage is not involved in the rate determining step.

In order to gain some insight into the kinetics of reactions of sulfido bimetallic clusters with nucleophiles, reactions of **1** and **2** with a series of phosphines were investigated.[6] These results showed that both **1** and **2** undergo CO displacement by an associative pathway, and in certain cases, an intermediate adduct, **3**, could be isolated in the reactions of cluster **1** with phosphines (Scheme 2). If the desulfurization reactions of **1** with thiols were to initially involve an association of the thiol with the cluster, then this step could be rate determining rather than the C−S bond cleavage. In this paper, we report the results of our investigation of the kinetics of the reaction of **1** with a series of thiols, and related reactions with aryl thiolate anions. This work

[⊗] Abstract published in *Advance ACS Abstracts,* January 15, 1997.

(1) (a) Topsøe, H.; Clausen, B. S.; Massoth, F. E. *Hydrotreating Technology*; Catalysis, Science and Technology, Vol. 11; Anderson, J. R.; Boudart, M., Eds., Springer-Verlag: New York, NY, 1996. (b) Chianelli, R. R.; Daage, M.; Ledoux, M. J. *Adv. Catal.* **1994**, *40*, 177−232. (c) Hoffman, H. L. *Hydrocarbon Process.* **1991**, *70*, 37. (d) Massoth, F. E. *Adv. Catal.* **1978**, *27*, 265.

(2) (a) Clausen, B. S.; Lengeler, B.; Topsøe, H. *Polyhedron* **1986**, *5*, 199. (b) Prins, R.; de Beer, V. H. J.; Somorjai, G. A. *Catal. Rev.-Sci. Eng.* **1989**, *31*, 1.

(3) Riaz, U.; Curnow, O.; Curtis, M. D. *J. Am. Chem. Soc.* **1994**, *116*, 4357.

(4) Riaz, U.; Curnow, O.; Curtis, M. D. *J. Am. Chem. Soc.* **1991**, *113*, 1416.

(5) Curtis, M. D.; Penner-Hahn, J. E.; Schwank, J.; Baralt, O.; McCabe, D. J.; Thompson, L.; Waldo, G. *Polyhedron* **1988**, *7*, 2411.

(6) Curnow, O. J.; Kampf, J. W.; Curtis, M. D.; Shen, J.-K.; Basolo, F. *J. Am. Chem. Soc.* **1994,** *116*, 224.

S0002-7863(96)02109-9 CCC: $14.00

Scheme 1

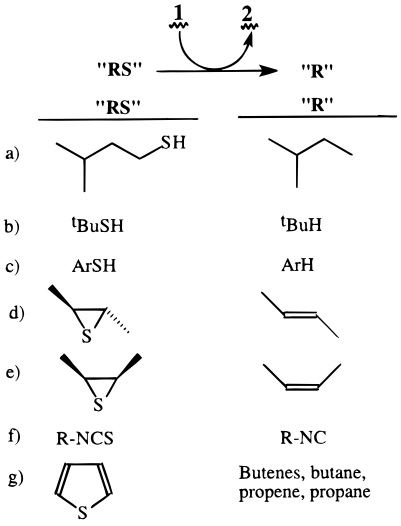

Scheme 2

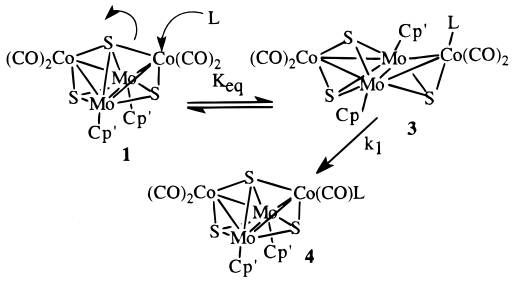

has allowed us to propose a mechanism for the aforementioned desulfurization reactions and to draw some parallels with the heterogeneously catalyzed HDS reaction. A preliminary account of this work has been published.[7]

Results

A series of aromatic and aliphatic thiols were allowed to react with **1** according to eq 1. Kinetic data were collected by

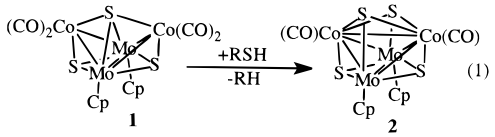

(1)

monitoring the disappearance of the CO stretching band centered at 1959 cm^{-1} for the cluster **1** (Figure 1) under pseudo-first-order conditions (excess of thiol). Plots of $\ln(A_t)$ (A_t is the absorbance of the 1959-cm^{-1} band) versus time were linear over several half-lives with correlation coefficients, r^2, greater than 0.991 for all of these plots. The slope of these straight lines yielded the pseudo-first-order rate constant k_{obs}. Dividing k_{obs} by the thiol concentration yielded the second-order rate constant k_2 (Table 1, Supporting Information). Plots of $\ln(k_2)$ versus $1/T$ produced straight lines, the slopes of which gave the activation energy (E_a) for the desulfurization reaction. Eyring plots, $\ln(k/T)$ versus $1/T$, produced straight lines, also, from which the activation parameters, $\Delta H^{\ddagger}$ and $\Delta S^{\ddagger}$, were obtained. These activation parameters are listed in Table 2. The rate of C_6H_5SH desulfurization under a CO atmosphere was the same within experimental error as the rate of desulfurization under a nitrogen atmosphere: $0.86(6) \times 10^{-3}$ versus 0.92×10^{-3} M^{-1} s^{-1}, respectively. This result is not consistent with any mechanism that requires CO dissociation prior to the rate determining step.

The linear plots for $\ln(A_t)$ versus time show that the rate of thiol desulfurization has a first-order dependence on cluster concentration. Plots of k_{obs} versus thiol concentration revealed the rate of the desulfurization reaction had a first-order dependence on thiol concentration (Figure 2). Thus, the rate law for the desulfurization of thiols mediated by cluster **1** is $d[\mathbf{2}]/dt = k_2[\mathbf{1}][\text{thiol}]$. The activation parameter $\Delta S^{\ddagger}$ was negative for all of the thiol desulfurization reactions. The value of $\Delta S^{\ddagger}$ ranged from $-5.0(1)$ cal/(mol·K) for C_6H_5SH to $-53.7(5)$ cal/(mol·K) for (*cyclo*-C_3H_5)CH_2SH. The rate law and the negative $\Delta S^{\ddagger}$ values are characteristic of an associative mechanism.

Phosphines also react with **1** via an associative mechanism and form an adduct with **1** at temperatures below −20 °C

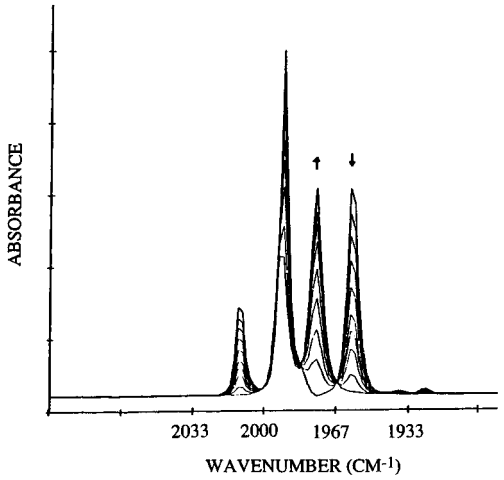

Figure 1. FT-IR spectra for the desulfurization of benzenethiol by cluster **1** in decalin at 119 °C.

Table 2. Activation Parameters for the Desulfurization of Aromatic and Aliphatic Thiols[a]

thiol	E_a (kcal/mol)	$\Delta H^{\ddagger}$ (kcal/mol)	$\Delta S^{\ddagger}$ (cal/mol K)
C_6H_5SH	28.0(6)	26.8(1)	−5.0(1)
p-ClC_6H_4SH	24(1)	23(2)	−12(2)
p-$CH_3C_6H_4SH$	23(1)	22(1)	−16(3)
p-$CH_3OC_6H_4SH$	20(2)	19(2)	−22(5)
$(CH_3)_3SH$	13.5(1)	12.9(1)	−39.1(2)
$CH_3(CH_2)_4SH$	8.2(1)	7.5(1)	−51.6(1)
(*cyclo*-C_3H_5)CH_2SH	7.5(2)	6.7(2)	−53.7(5)

[a] Standard deviations are given in parentheses.

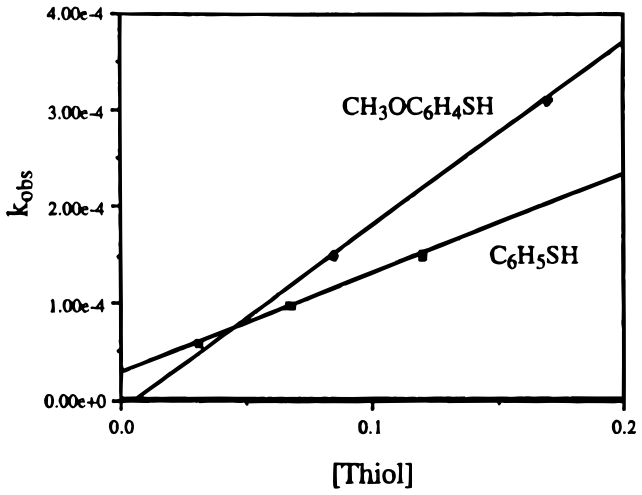

Figure 2. Plot of k_{obs} vs. thiol concentration.

(7) Druker, S. H.; Curtis, M. D. *J. Am. Chem. Soc.* **1995**, *117*, 6366.

(Scheme 2).[6] The typical activation parameters for associative phosphine adduct formation were found to be $\Delta H^{\ddagger} \approx 6$ kcal/mol and $\Delta S^{\ddagger} \approx -28$ cal/(mol·K).[6] These activation parameters are similar to the average activation parameters for the thiol desulfurization reactions: $\Delta H^{\ddagger} \approx 9$ kcal/mol, $\Delta S^{\ddagger} \approx -48$ cal/(mol·K) for aliphatic thiols and $\Delta H^{\ddagger} \approx 23$ kcal/mol, $\Delta S^{\ddagger} \approx -14$ cal/(mol·K) for aromatic thiols. This process is associative, also. The overall rate law for the ligand substitution reaction depicted in Scheme 2 is

$$\mathrm{d[product]}/\mathrm{d}t = (k_1 K_{eq}[\mathbf{L}]([\mathbf{1}] + [\mathbf{1}\cdot\mathbf{L}]))/(1 + K_{eq}[\mathbf{L}]) \quad (2)$$

In the limiting case, where $K_{eq}[\mathbf{L}] \ll 1$, eq 2 reduces to a rate law that is first order in ligand and first order in cluster. Thiols are weaker nucleophiles than phosphines; therefore, it is reasonable to assume that K_{eq} for the reaction of **1** with thiols is small compared to the value for phosphines. As a result, the rate law for the thiol desulfurization reactions can be considered to be derived from a limiting case of the mechanism shown in Scheme 2.

The rate of thiol desulfurization increased in the following order: C_6H_5SH < *p*-ClC_6H_4SH, *p*-$CH_3C_6H_4SH$ < *p*-$CH_3OC_6H_4SH$ < $(CH_3)_3CSH$ < *n*-$C_5H_{11}SH$, (*cyclo*-$C_3H_5)CH_2SH$. Aliphatic thiols reacted faster than aromatic thiols, and primary thiols reacted faster than tertiary thiols. Aliphatic groups donate electron density through inductive effects, while an aromatic group acts as an electron-withdrawing group. Therefore, the sulfur atom is more nucleophilic in aliphatic thiols than in aromatic thiols. Since aliphatic thiols are better nucleophiles, they react faster than aromatic thiols with **1** to form the adduct that leads to desulfurization. The faster rate of reaction for primary thiols versus tertiary thiols is also typical for an S_N2 type of reaction. The bulky *tert*-butyl group causes steric crowding in the transition state, and the crowding slows down the rate of the reaction. The increased rate of reaction for the more nucleophilic and less sterically hindered thiols suggests that the rate determining step in the desulfurization reaction is coordination of the thiol to **1**.

Trends in the activation parameters $\Delta H^{\ddagger}$ and $\Delta S^{\ddagger}$ can provide information on the structure of the transition state complex that forms when thiols react with **1**. For large positive values of $\Delta H^{\ddagger}$ and $\Delta S^{\ddagger}$, the transition state complex is formed late in the reaction, and the transition state complex has a large degree of bond breaking. Small values of $\Delta H^{\ddagger}$ and negative $\Delta S^{\ddagger}$ values indicate that the transition state complex is formed early in the reaction and resembles the reactants, i.e., less bond breaking and more bond making in the transition state complex.[8] Large, negative $\Delta S^{\ddagger}$ values were reported for the reaction of **1** with phosphines.[6] Consequently, it is proposed that the magnitude of $\Delta S^{\ddagger}$ for the thiol reactions is a measure of the relative amount of Co−thiol bond formation and Co−(μ_4-S) bond breakage in the transition state complex (cf. Scheme 2). A large negative $\Delta S^{\ddagger}$ value for the thiol desulfurization reactions implies a high degree of thiol−Co bond formation with little Co−(μ_4-S) bond breakage, whereas a less negative $\Delta S^{\ddagger}$ means a large amount of Co−(μ_4-S) bond breaking precedes thiol−Co bond formation.

The value of $\Delta H^{\ddagger}$ for the thiol desulfurization reactions increased in the order *n*-$C_5H_{11}SH$, (*cyclo*-$C_3H_5)CH_2SH$ < $(CH_3)_3CSH$ < *p*-$CH_3OC_6H_4SH$ < *p*-ClC_6H_4SH, *p*-$CH_3C_6H_4SH$ < C_6H_5SH (Table 2), and the values of $\Delta S^{\ddagger}$ became less negative in this order. Small positive $\Delta H^{\ddagger}$ values and large negative $\Delta S^{\ddagger}$ values were typical for the aliphatic thiol reactions. This suggests a transition state in which there is a high degree of Co−thiol bond formation, but relatively little Co−(μ_4-S) bond breaking. The reverse order in the activation parameters for the aromatic thiols, i.e., large positive $\Delta H^{\ddagger}$ values and small negative $\Delta S^{\ddagger}$ values, indicates that in these transition states the Co−thiol bond is weaker (consistent with the lower basicity of the aromatic thiols) and that there is a higher degree of Co−(μ_4-S) bond cleavage as in adduct **3**, Scheme 2.

These interpretations suggest that the rate determining step of the thiol desulfurization reaction (eq 1) is the coordination of the thiol to the cluster, and the cleavage of the C−S bond then occurs rapidly. Regardless of the detailed mechanism of the C−S bond cleavage step, the effective C−S bond dissociation energy (BDE) in the reaction depicted by eq 1 cannot exceed the activation energy for the rate determining step, i.e. the C−S BDE is ≤ ca. 20 kcal/mol. This value is only about 25% of the value for the C−S BDE in aromatic thiols![9] Thus, coordination of the thiol to the cluster results in a substantial weakening of the C−S bond energy. In order to better study the C−S bond cleavage step, it is necessary to change the rate determining step. We reasoned that thiolate anions should coordinate readily to cluster **1** and the slow step of the desulfurization might then become the C−S bond cleavage itself.

Reactions of 1 with Thiolate Anions. The reaction of **1** with $(NEt_4)(SC_6H_4CH_3)$ in acetone-d_6 was followed by ^{1}H-NMR spectroscopy. At 213 K, an immediate reaction occurred, all of **1** was consumed, and a red adduct **5a** was formed. The ^{1}H-NMR spectrum revealed a set of resonances characteristic of one ABCD pattern for the Cp′ protons and a single resonance for the Cp′ methyl groups. The spectral pattern of **5a** was analogous to the proton spectrum of the trimethylphosphine adduct of **1** (**3**, Scheme 2, L = Me_3P).[6]

The adduct **5a** was rapidly converted to a new compound (**5b**) as the temperature of the solution was raised to 266 K. The ^{1}H-NMR spectrum of **5b** at 266 K had seven multiplets in the Cp′H region that integrated in the ratio of 1:2:1:1:1:1:1, i.e. two ABCD patterns appeared to be present. Also, two singlets were observed for the Cp′ methyl protons. This spectral pattern indicated **5b** had C_1 symmetry. Adduct **5a** was not regenerated when the temperature of the solution was again lowered to 213 K.

The same anionic species, **5b**, formed directly from **1** and $[(C_6H_5CH_2)N(CH_3)_3]$ $[SC_6H_4CH_3]$ at room temperature. The deep red color of the thiolate adduct of **5a** formed initially, but within seconds the color changed to olive-green. The IR spectrum of the olive-green solution was dominated by two new CO stretching bands centered at 1963 and 1912 cm^{-1}. The frequency of the lower wavenumber peak was dependent on the type of thiolate: for aliphatic thiolates, the lower frequency CO stretching band was centered at 1900 cm^{-1}. Peaks characteristic of **1** were visible in the solution IR spectrum even in the presence of excess thiolate (vide infra). Dark green crystals of the product $[(C_6H_5CH_2)N(CH_3)_3][\mathbf{1}\cdot SC_6H_4CH_3]$ ($[BnNMe_3][\mathbf{5b}]$) were isolated. Unfortunately, all attempts to grow X-ray quality single crystals were unsuccessful. A ^{1}H-NMR spectrum recorded at 249 K confirmed that the structure of **5b** was identical to the tetraethylammonium salt obtained from **5a** by rearrangement at low temperature.

The decreased symmetry of **5b**, as evidenced in the ^{1}H-NMR spectrum, suggested that the thiolate ligand had rearranged from a terminal position in **5a** to a bridging position over a Co−Mo bond in **5b**. In fact, judging from the paucity of terminal thiolates vs. bridging thiolates in multinuclear complexes, one can conclude that the bridging mode is highly favored over the terminal bonding mode whenever the latter is possible.[10a−c]

(8) Morrison, R. T.; Boyd, R. N. *Organic Chemistry*, 5th ed.; Allyn and Bacon, Inc.: Boston, 1987; p 68.

(9) The homolytic bond dissociation energy was calculated using thermochemical data listed in the reference: Griller, D.; Kanabus-Kaminsks, J. M.; Maccoll, A. J. *J. Mol. Struct. (Theochem)* **1988**, *163*, 125.

Scheme 3

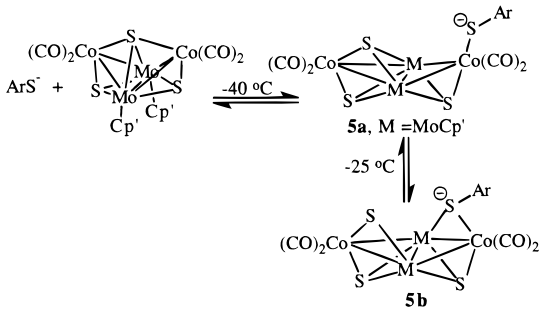

As mentioned above, cluster **1** was detected in the reaction mixture even in the presence of excess thiolate. The amount of **1** present was dependent on the solubility of the thiolate salt. For example, the reaction of $NaSC_6H_4CH_3$ with **1** in CH_3CN yielded approximately a 50:50 mixture of **1** to the thiolate complex of **1**. This ratio was qualitatively determined by comparing the intensity of the 1988 cm^{-1} band characteristic of **1** with the 1912 cm^{-1} band characteristic of the product. Sodium thiolates have a very low solubility in CH_3CN, and the addition of 15-crown-5 ether substantially increases their solubility. When 15-crown-5 ether was added to the $NaSC_6H_4$-CH_3/**1** mixture, only a trace amount of **1** was detected in the solution IR spectrum. These results show that **5a** is a kinetic product in the addition of thiolate anions to cluster **1**, and the thermodynamic product, **5b**, is in equilibrium with free thiolate anion. Therefore, **5b** is almost certainly in equilibrium with **5a** also, although the amount of the latter is so small that it is not detected in our NMR experiments. These transformations are shown in Scheme 3.

An alternative product with C_1 symmetry that could be formed in the reaction of a thiolate anion with cluster **1** is the CO substitution product, **6** (eq 3), analogous to the phosphine

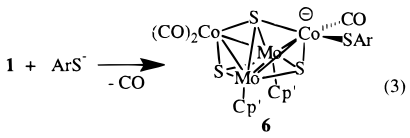

(3)

substituted clusters shown in Scheme 2. Since the formation of **6** involves the loss of a CO ligand, it is unlikely that an equilibrium would be established between **6** and free thiolate under our experimental conditions. Although the elemental analysis of **5b** is consistent with its formula, the differences in the calculated elemental percentages between **5b** and **6** are too small to reliably differentiate between these two species. The parent ion peak in the electrospray ionization mass spectrum (ESI-MS) of **5b** was observed at *m*/*z* 799 (Figure 3) when the inlet was held at 35 °C. This mass corresponds to the mass of the anion, $Cp'_2Mo_2Co_2S_3(CO)_4(SC_6H_4CH_3)^-$. When the ESI-MS of **5b** was collected at 60 °C instead of at 35 °C, the parent ion peak was observed at *m*/*z* 771, corresponding to the loss of a carbonyl ligand, i.e. the substituted derivative, **6**.

Further confirmation that the adduct assigned formula **5b** is not the CO-substituted derivative **6** was obtained when a trace amount of **6** was isolated during an attempt to grow crystallographic quality crystals of **5b**. A few well formed crystals of **6** were picked out of the mass of smaller needles of **5b**

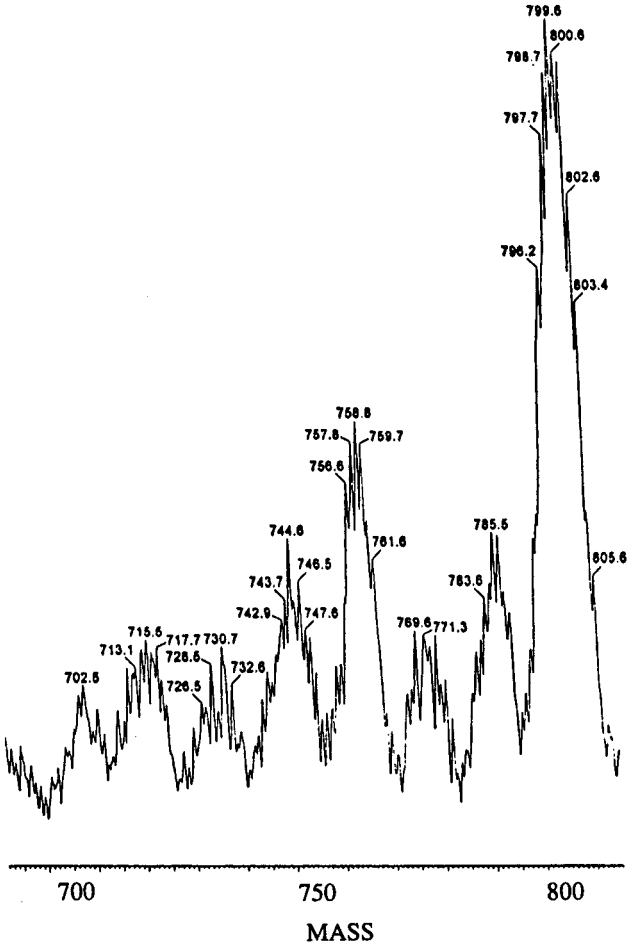

Figure 3. Electrospray ionization−mass spectrum (ESI-MS) of cluster anion **5b**.

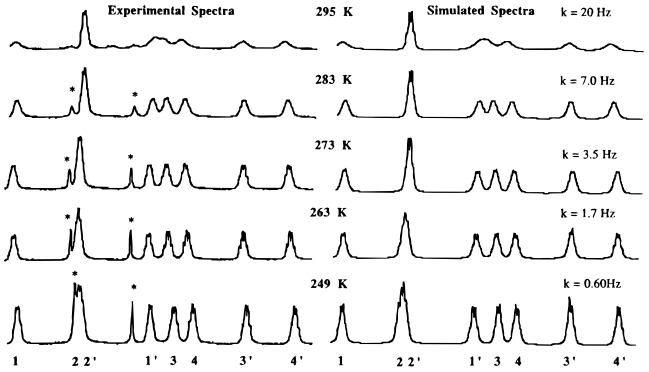

Figure 4. Variable-temperture ^{1}H-NMR spectra of the adduct of *p*-toluenethiol and **1** in CD_3CN.

(analyzed by elemental analysis, ESI-MS, and ^{1}H NMR) and identified by a single crystal X-ray analysis (the structure will be reported separately).[10d] Attempts to directly synthesize **6** were unsuccessful: photolysis of **5b** resulted in complete degradation, and heating a solution of **1** and $[(C_6H_5CH_2)$-$N(CH_3)_3][SC_6H_4CH_3]$ resulted in desulfurization of the thiolate and the formation of the cubane cluster anion, **7** (see below).

VT-NMR of 5b. Variable-temperature ^{1}H-NMR experiments revealed the thiolate complexes of **1**, e.g. **5b**, are stereochemically nonrigid and show an interesting mobility of the coordinated thiolate ligand. At −24 °C, the Cp′ rings were inequivalent as evidenced by the two ABCD patterns for the Cp′H protons and two signals for the Cp′CH_3 protons (Figure 4). A 2D-COSY NMR spectrum of **5b** allowed the coupling pattern for the ring protons to be determined (Figure 5). The proton

(10) (a) Seela, J. L.; Huffman, J. C.; Christou, G. *J. Chem. Soc., Chem. Commun.* **1987**, 1258. (b) Bernatis, P.; Haltiwanger, R. C.; Rakowski Dubois, M. *Organometallics* **1992**, *11*, 2435. (c) Cotton, F. A.; Wilkinson, G. *Advanced Inorganic Chemistry*, 5th ed.; John Wiley & Sons Inc.: 1988; p 531. (c) Curtis, M. D.; Druker, S. H.; Goossen, L.; Kampf, J. W. *Organometallics* In press.

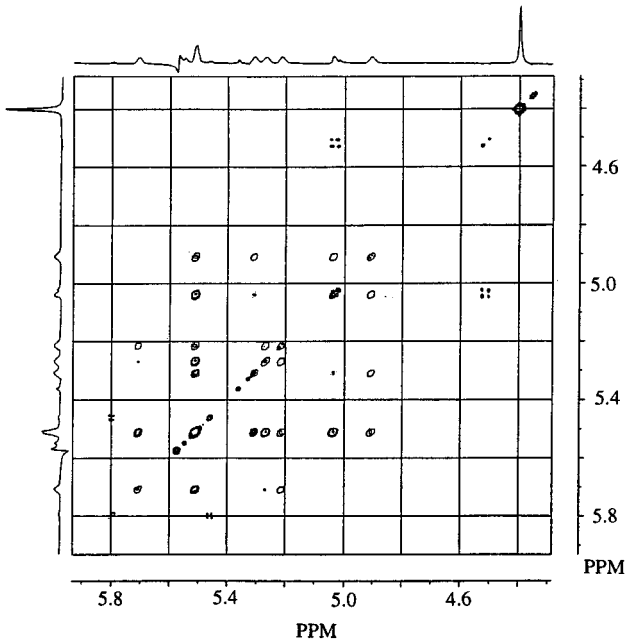

Figure 5. COSY 2D-NMR spectrum of **5b** in CD_3CN.

resonances at δ 5.51, 5.31, 5.01, and 4.86 form one ABCD pattern; the resonances at δ 5.70, 5.51, 5.22, and 5.18 form the second ABCD pattern. At −10 °C, the Cp′H proton signals were broad and the Cp′CH_3 signals began to merge. At +22 °C, the resonances for the Cp′H protons were broad and coalescing, and only a single peak was observed for the Cp′CH_3 protons.

A synchronized movement of the thiolate and μ_2-bridging sulfide ligands on the surface of the cluster can explain the variable-temperature NMR behavior of compound **5b**. Three likely mechanisms for the fluxional process can be envisioned: (1) the thiolate and sulfide cross the Mo−Mo bond axis, (2) the thiolate and sulfide cross the Co−Co bond axis, or (3) a combination of these two motions. Motion (1) generates a time average mirror plane that bisects the Cp′ groups, leaves the Cp′ methyl groups inequivalent, but converts the two ABCD patterns to two A_2B_2 patterns for the Cp′H protons. Motion (2) generates a time average mirror plane that bisects the Mo−Mo bond, renders the two Cp′ methyl groups equivalent, but leaves the Cp′ groups diasterotopic (hence their ABCD pattern). Finally, the combination of these two motions produces an average C_{2v} symmetry so that one A_2B_2 pattern for the Cp′H protons and one Me signal would be observed.

The reactivity of **5b** (see below) precluded spectra from being recorded in the fast exchange limit, nonetheless, pathway (1) was ruled out. At +22 °C, only a single peak was observed for the Cp′CH_3 protons contrary to the prediction of inequivalent Me groups of motion (1). The Cp′H spectra were simulated with the program DNMR5. Several models were tested, but only the one involving the spin interchanges required by motion (2) gave computed spectra that agreed with the experimental results at low temperatures. At higher temperatures, it was apparent from the modeling that a second fluxional process was beginning to influence the peak shapes in a manner consistent with interchange of spins expected for motion (2). However, the onset of sample decomposition precluded accurate modeling of this process. Thus, the VT-NMR spectra are consistent with the atomic motions depicted in Scheme 4.

The activation barrier associated with the thiolate crossing the Co−Co bond axis was determined from the rate constants shown in Figure 4, obtained from the DNMR modeling. A plot

Scheme 4

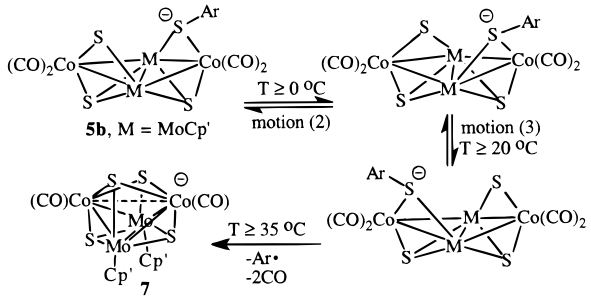

of ln(k) vs. 1/T yielded a straight line, the slope of which gave a value of 10(1) kcal/mol for the Arrhenius activation barrier, E_a, for the fluxional process. An Eyring plot gave values for the activation parameters $\Delta H^{\ddagger}$ and $\Delta S^{\ddagger}$ of 9 kcal/mol and −21.4 cal/(mol·K), respectively.

Desulfurization of Thiolate Anions. Our expectation that the thiolate anions would bind readily to the cluster **1** was confirmed by the results described above, and the thiolate adduct was found to decompose at relatively low temperatures. This "decomposition" reaction resulted in the desulfurization of the bound thiolate. In refluxing CD_3CN, the adduct **5b** was consumed, and a new organometallic complex, **7**, was formed (Scheme 4). Three organic products were detected (^{1}H-NMR, GC-MS): toluene-d_1 (m/z 93), $(C_6H_5CH_2)N(CH_3)_2$ (m/z 135), and $CH_3SC_6H_4CH_3$ (m/z 138).

The identification of toluene-d_1 and **7** provided the first insight into the mechanism by which **1** activates C−S bond cleavage. Deuterium incorporation into the organic product is consistent with the formation of the *p*-tolyl radical by homolysis of the C−S bond, and subsequent abstraction of the deuterium from the solvent by the radical (eq 4).

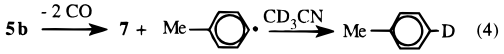

The remaining two organic products, $(C_6H_5CH_2)N(CH_3)_2$ and $CH_3SC_6H_4CH_3$, result from the nucleophilic attack of the thiolate anion on the benzyltrimethylammonium cation present in the reaction mixture. This reaction was confirmed by a separate control experiment (heating a solution of $[(C_6H_5CH_2)N(CH_3)_3]$-$[SC_6H_4CH_3]$ in CD_3CN). As expected, no toluene-d_1 was detected in the control experiment.

The desulfurization of ^{t}BuSNa was also consistent with a free radical mechanism for C−S bond cleavage. Cluster **1** was allowed to react with ^{t}BuSNa in refluxing CH_3CN. The organometallic compound that formed was **7**. The only organic product that was detected (GC-MS) was isobutane. No isobutene was observed in the mixture. If the C−S bond were cleaved heterolytically to produce the *tert*-butyl cation, then some isobutene would have been produced.[11]

To provide further support for the proposed homolytic cleavage of the C−S bond during the cluster-mediated desulfurization of thiols, the desulfurization of a "radical clock" reagent, cyclopropylmethyl thiolate, was examined. It has been established that the cyclopropylmethyl radical rapidly ($k = 61 \times 10^7$ s^{-1} at 80 °C) ring opens to form the butenyl radical,[12] which, in acetonitrile-d_3, should form 1-butene-d_1. In fact, 1-butene-d_1 (identified by ^{1}H-NMR and GC-MS) was measured as the

(11) Coucouvanis, D.; Al-Ahmad, S.; Kim, C. G.; Koo, S.-M. *Inorg. Chem.* **1992**, *31*, 2996.

(12) (a) Franceschi, G.; Foglio, M.; Masi, P.; Suarato, A.; Palamidessi, G.; Bernardi, L.; Arcamone, F. *J. Am. Chem. Soc.* **1977**, *99*, 250. (b) San Filippo, J., Jr.; Silbermann, J.; Fagan, P. J. *J. Am. Chem. Soc.* **1978**, *100*, 4834. (c) Beckwith, L. J. A.; Bowry, V. W. *J. Am. Chem. Soc.* **1994**, *116*, 2710.

Scheme 5

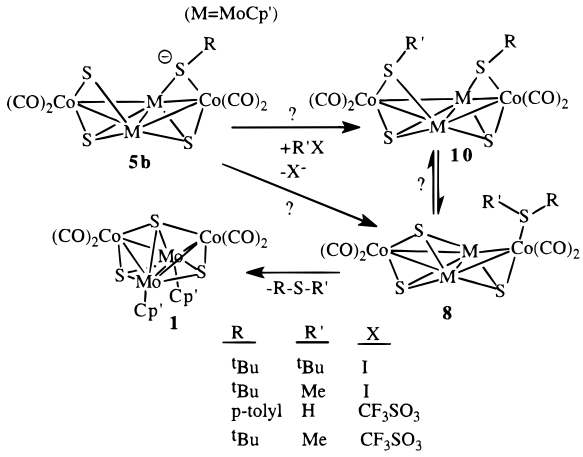

Scheme 6

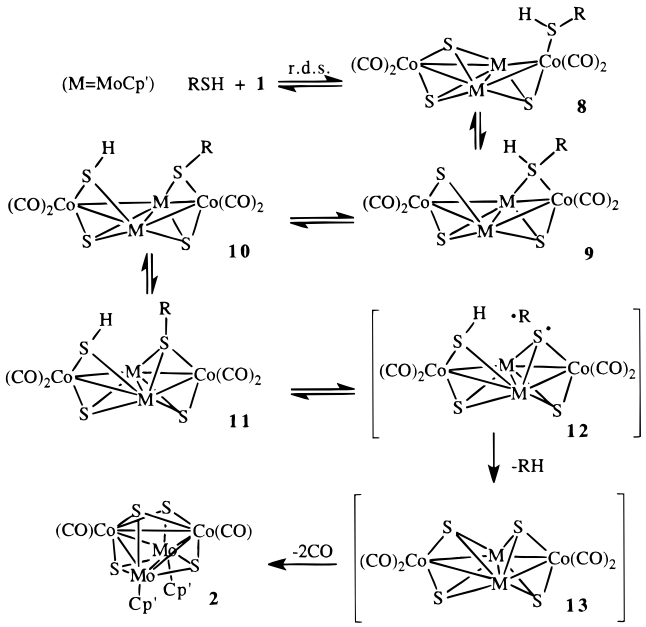

sole organic product and cluster anion **7** was detected by IR after refluxing a solution of $LiSCH_2(cyclo\text{-}C_3H_5)$ and cluster **1** in deuterated acetonitrile for 2 h. This result is entirely consistent with homolysis of the C−S bond in the coordinated thiolate anion.

Desulfurization of cyclopropylmethanethiol by **1** in toluene-d_8 or acetonitrile-d_3 also led to the rearrangement characteristic of the cyclopropylmethyl radical. With the thiol, however, there was no deuterium incorporated into the 1-butene product. This implies that the rate of H-atom abstraction from either free thiol or a thiol−cluster complex is much faster than the rate of abstraction of deuterium from the solvent. Other radical clocks are currently under investigation in order to clarify this point.[13]

Reaction of Thiolate−Cluster Adducts with Electrophiles. Several attempts were made to synthesize a thiol−cluster or an organic sulfide−cluster complex at low temperatures by protonation or alkylation, respectively, of the thiolate−cluster adducts (Scheme 5). The goal of this exercise was to synthesize one of the putative intermediates, **8**−**10** (Scheme 6), in the mechanism proposed for the desulfurization of thiols mediated by cluster **1** (see Scheme 6). In all cases, it was found that these reactions gave as products the starting cluster **1** and the free thiol or sulfide, R−S−R′. We saw no evidence for the formation of products, e.g. **8**−**10**. Apparently, the thiolato S-atom is the site of electrophilic attack (or the electrophile is rapidly transferred to the thiolato S-atom), and the thiol or sulfide, R−S−R′, rapidly dissociates from the cluster. This result is, of course, fully consistent with the equilibrium depicted in Scheme 2 lying far to the left when L = RSH, as deduced from the kinetics of the reaction of **1** with thiols.

(13) Dungey, K. M.; Curtis, M. D. *J. Am. Chem. Soc.* In press.

Discussion

The results presented above show that coordination of thiolate or thiol ligands to the Mo/Co/S cluster **1** leads to activation of the C−S bond to homolytic cleavage. Homolytic cleavage of C−S bonds in thiolate metal complexes has been observed by other research groups.[11,14,15] The discovery that **1** activates C−S bonds toward homolysis also helped to clarify the results of a reaction reported by Curnow et al.[3] An unknown organic compound, **U1**, with a mass of 134 g/mol was detected by mass spectral analysis when **1** was allowed to react with benzenethiol under CO pressure in *p*-xylene solvent.[3] It is now clear that **U1** was *p*-tolylacetaldehyde, formed from the reaction of the *p*-methylbenzyl radical with CO followed by a H-atom transfer. The *p*-methylbenzyl radical itself was formed by a H-atom abstraction from the solvent by the initially produced phenyl radical. The mass spectral fragmentation pattern of **U1** was identical to authentic *p*-tolylacetaldehyde, thus confirming this assignment.

The geometry of the thiolate adducts could be inferred from the low temperature NMR spectra, and the observed fluxional behavior gives some valuable clues about the molecular motions of the thiol group on the surface of the cluster. These observations allow us to propose the mechanism for the cluster-mediated desulfurization shown in Scheme 6. In this scheme, the rate determining step is the initial coordination of the thiol to the cluster **1** to form adduct **8** with a thiol terminally coordinated to a Co atom. The thiol then bends over and bridges the Co−Mo bond, displacing a μ_3-sulfide bond and forming a μ_2-sulfide−μ_2-thiol complex (**9**). The μ_2-coordination increases the acidity of the thiol proton which is then transferred to the μ_2-sulfide ligand (**10**). The μ_2-thiolate in **10** has a lone pair with which it can form an additional bond to become μ_3-bound (**11**). We propose that the μ_3-mode of coordination leads to the activation of the C−S bond to homolytic cleavage by decreasing the C−S bond dissociation energy (BDE) to around 20−25 kcal/mol. A BDE is simply the difference in the final state and initial state energies of a dissociative reaction. The more stable the final state, the lower the BDE. A comparison of the final states in the reactions shown in eqs 5 and 6 reveals

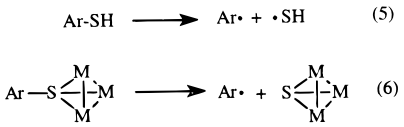

the reason why coordination of the thiolate to the cluster results in a lower BDE. Simply put, the μ_3-coordinated sulfide is in a much more stable bonding situation than is the S atom in the HS• radical. The conversion of the $M_3(SR)$ group to a $M_3(S)$ group represents a net oxidation of the cluster (eq 6). The effect of the oxidation is spread out over the entire 4-atom ensemble instead of being localized on the S atom as in eq 5. C−S bond activation by bridge bonding in clusters or on metal surfaces

(14) (a) Adams, R. D.; Horváth, I. T.; Mathur, P.; Segmüller, B. E. *Organometallics* **1983**, *2*, 996. (b) Adams, R. D.; Pompeo, M. P. *Organometallics* **1992**, *11*, 103.

(15) Luh, T.-Y.; Ni, Z.-J. *Synthesis* **1990**, 89.

should be a general phenomenon and may explain the catalytic action of HDS catalysts.

Mechanistic Aspects of Metal-Promoted C−S Bond Cleavage Reactions. The cleavage of the C−S bond is central to catalytic HDS desulfurization and to the application of desulfurization reactions to synthetic organic problems. Luh and coworkers[15] have developed several transition metal-mediated desulfurization reactions for synthetic applications, but the exact nature of the active species and the detailed mechanism(s) of the C−S bond cleavage are obscure. Similarly, the mechanism of the C−S bond cleavage over commercial HDS catalysts is still completely unknown in spite of the extensive research on these catalysts (ref 1a lists over 1500 references on HDS catalysis). Overall reaction pathways have been worked out in several instances, e.g. benzothiophene → dihydrobenzothiophene → ethylbenzene, but the mechanisms of the individual reactions are not known.[16] Consequently, the role of the promoter element, Co or Ni, is also completely unknown (there are at least 24 proposals in the literature for the cause of the promoter effect!).[17]

Given the complexity of supported HDS catalysts, much attention has been focused on modeling the catalyst−substrate interactions by organometallic and coordination complexes of thiophene and other organic sulfur compounds. Thiophene and its derivatives have received greater attention because these molecules are among the more difficult to desulfurize.[18,19] The strength of the modeling approach lies in the fact that detailed bonding modes and reaction mechanisms can be developed readily for the model and then applied to the complex catalyst. The transfer of mechanistic ideas, etc., is most readily achieved when the model systems closely resemble the catalyst, both in composition and structure.

The results of the present work show that homolytic cleavage of the C−S bond must be considered as a possible reaction pathway whenever a thiol or thiolate intermediate is generated on the catalyst surface. Homolytic C−S cleavage has been observed on thiolate−cluster complexes previously.[14,20] A low oxidation state metal also promotes C−S bond homolysis in mononuclear thiolate complexes.[21] This is understandable since conversion of an M−SR complex to an M−S complex by loss of a neutral radical, R•, represents a formal oxidation of the metal.

Low valent, electron rich metal complexes promote oxidative addition into the C−S bond.[22−24] Oxidative insertion creates a metal thiolate. Such thiolate intermediates may aggregate to form clusters or higher nuclearity complexes with the thiolate sulfur in bridging environments, i.e. conditions conducive to C−S bond homolysis may be set up by an initial C−S oxidative insertion step. Jones et al. have observed the formation of dimers and clusters in the reactions of mononuclear complexes with thiophene.[22]

Scheme 7

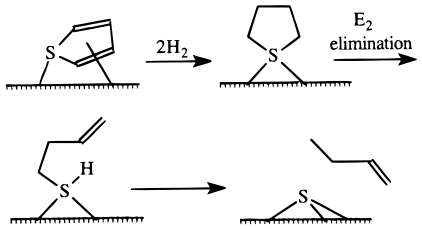

Hydrogenation of a C═C double bond, followed by an E_2 elimination reaction, is another possible pathway to the formation of thiolate complexes. This pathway is illustrated in Scheme 7 for thiophene. Final release of 1-butene could occur by C−S bond homolysis. This pathway rationalizes the primary formation of 1-butene observed during HDS of thiophene over CoMoS catalysts.[5,25−27]

Similarly, in the HDS of benzothiophene (BT), partial hydrogenation to dihydrobenzothiophene followed by an E_2 elimination would produce a vinylbenzene thiolate (Scheme 8). C−S bond homolysis would release styrene which could be hydrogenated to ethylbenzene. Both products are found in the HDS of BT.

These two examples show just two of several pathways that could lead to the formation of thiolate surface intermediates during the HDS of thiophenic compounds. Hence, reaction mechanisms that are demonstrated for thiols have implications for the HDS of thiophenes. In fact, C−S bond homolysis has not been excluded as a possible mechanism for the final C−S bond scission even in reactions where oxidative addition is the first step that leads to initial products with M−S−C bonds.[24] Note: the site of initial adsorption or hydrogenation of thiophenic compounds may differ from the site(s) for C−S bond cleavage.[1]

Latent Vacancies and Sulfur Mobility. The mechanism shown in Scheme 5 may have a further implication for the role of the Co-promoter atom located at the edges of the MoS_2 slabs in the "CoMoS" phase catalyst.[1a] EXAFS measurements have indicated that the cobalt atoms active in promotion are capable of variable coordination number and variable oxidation states,

(16) Girgis, M. J.; Gates, B. C. *Ind. Eng. Chem. Res.* **1991**, *30*, 2021.
(17) See reference 1a, p 163.
(18) (a) Angelici, R. J. *Acc. Chem. Res.* **1988**, *21*, 387. (b) Chen, J.; Angelici, R. J. *Organometallics* **1990**, *9*, 879, 849. (c) Benson, J. W.; Angelici, R. J. *Organometallics* **1993**, *12*, 680. (d) Benson, J. W.; Angelici, R. J. *Organometallics* **1992**, *11*, 922. (e) Sauer, N. N.; Markel, E. J.; Schrader, G. L.; Angelici, R. J. *J. Catal.* **1989**, *117(1)*, 295−7. (f) Robertson, M. J.; Day, C. L.; Jacobson, R. A.; Angelici, R. J. *Organometallics* **1994**, *13*, 179. (g) Chen, J.; Daniels, L. M.; Angelici, R. J. *Organometallics* **1996**, *15*, 1223. (h) Chen, J.; Young, V. G. J.; Angelici, R. J. *Organometallics* **1996**, *15*, 1414.
(19) (a) Rauchfuss, T. B. *Prog. Inorg. Chem.* **1991**, *39*, 260. (b) Luo, S.; Rauchfuss, T. B.; Gan, Z. *J. Am. Chem. Soc.* **1993**, *115*, 4943. (c) Luo, S.; Ogilvy, A. E.; Rauchfuss, T. M.; Rheingold, A. L.; Wilson, S. R. *Organometallics* **1991**, *10*, 1002. (d) Krautscheid, H.; Feng, Q.; Rauchfuss, T. B. *Organometallics* **1993**, *12*, 3273. (e) Feng, Q.; Krautscheid, H.; Rauchfuss, T. R.; Skaugset, A. E.; Venturelli, A. *Organometallics* **1995**, *14*, 297−304.
(20) (a) Adams, R. D. *Chem. Rev.* **1995**, *95*, 2587. (b) Adams, R. D.; Horvath, I. T. *Prog. Inorg. Chem.* **1985**, *33*, 127. (c) Adams, R. D.; Pompeo, M. P.; Wu, W.; Yamamoto, J. H. *J. Am. Chem Soc.* **1993**, *115*, 8207 and references therein. (d) Adams, R. D. *Polyhedron* **1985**, *4(12)*, 2003−26. (e) Adams, R. D.; Pompeo, M. P.; Wu, W.; Yamamoto, J. H. *J. Am. Chem. Soc.* **1993**, *115*, 8207.
(21) Kim, J. S.; Reibenspies, J. H.; Darensbourg, M. Y. *J. Am. Chem. Soc.* **1996**, *118*, 4115.
(22) (a) Myers, A. J.; Jones, W. D.; McClements, S. M. J. *Am. Chem. Soc.* **1995**, *117*, 11704. (b) Jones, W. D.; Chin, R. M. *J. Am. Chem. Soc.* **1994**, *116*, 198. (c) Jones, W. D.; Chin, R. M. *Organometallics* **1992**, *11*, 2698. (d) Rosini, C. P.; Jones, W. D. *J. Am. Chem. Soc.* **1992**, *114*, 10767. (e) Dong, L.; Duckett, S. B.; Ohman, K. F.; Jones, W. D. *J. Am. Chem. Soc.* **1992**, *114*, 151. (f) Jones, W. D.; Chin, R. M. *J. Am. Chem. Soc.* **1992**, *114*, 9851.
(23) Harris, S. *Organometallics* **1994**, *13*, 2628.
(24) (a) Bianchini, C.; Meli, A. *J. Chem. Soc., Dalton Trans.* **1996**, 801. (b) Bianchini, C.; Meli, A.; Perizzini, M.; Vizza, F.; Herrera, V.; Sanchez-Delgado, R. A. *Organometallics* **1994**, *13*, 721. (c) Bianchini, C.; Meli, A.; Peruzzini, M.; Vizza, F.; Moneti, S.; Herrera, V.; Sanchez-Delgado, R. A. *J. Am. Chem. Soc.* **1994**, *116*, 4370. (d) Bianchini, C.; Jimenez, M. V.; Meli, A.; Moneti, S.; Vizza, F.; Herrera, V.; Sanchez-Delgado, R. A. *Organometallics* **1995**, *14*, 2342. (e) Bianchini, C.; Meli, A.; Peruzzini, M.; Vizza, F.; Frediani, P.; Herrera, V.; Sanchez-Delgado, R. A. *J. Am. Chem. Soc.* **1993**, *115*, 2731. (f) Bianchini, C.; Meli, A.; Peruzzini, M.; Vizza, F.; Frediani, P. H.; Sanchez-Delgado, R. A. *J. Am. Chem. Soc.* **1993**, *115*, 7505.
(25) Schulz, H.; Do, D.-V. *Bull. Soc. Chim. Belg.* **1984**, *93*, 645.
(26) Moser, W. R.; Rossetti, G. A.; Gleaves, J. T.; Ebner, J. R. *J. Catal.* **1991**, *127*, 190.
(27) Startsev, A. N.; Burmistrov, V. A.; Yermakov, Yu. I. *Appl. Catal.* **1988**, *45*, 191.

Scheme 8

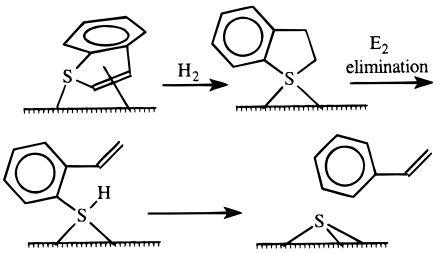

and are the sites for initial adsorption of thiophene.[27−29] Our results show that the Co atom in cluster **1** is the site of initial attack by nucleophiles, but the coordination of the Co does not change because the Co−(μ_4-S) bond is displaced.

We define the Co sites in cluster **1** as *latent vacancies* since they react as if they have a vacancy in their coordination shell, yet, in their "resting state", a neighboring S atom "fills" the vacancy. The concept of a latent vacancy is appealing since the resting state of the latent vacancy has a lower energy than that of a bare, uncompensated vacancy. In cluster **1**, the weaker Co−S bond, compared to the stronger Mo−S bond, allows for substrate molecules to displace a Co−S−M bridge bond and bind to the catalyst surface. Similar behavior could occur at the promoted sites in the CoMoS phase. The presence of latent vacancies may also explain why the number of vacancies determined by titrating the surface of HDS catalysts depends on the titrant (adsorbate).[30] Titrants capable of displacing Co−S bonds "find" more sites than those that cannot displace Co−S bridge bonds.

Latent vacancies on a catalyst surface would also influence the adsorption of substrate molecules and, hence, their rates of desulfurization. Electron releasing groups ortho or para (but not meta) to the thiol group in substituted benzenethiols enhance the rate of desulfurization over heterogeneous CoMoS catalysts.[31] We have shown in this work that electron releasing groups in the para position in aryl thiols bind better to the cluster and increase the rate of desulfurization. Thus, cluster **1** models the selectivity of the heterogeneous catalyst for aryl thiols, lending further support for the concept of latent vacancies.

The observed fluxional motions of the thiolate groups over the face of the Co/Mo/S cluster parallel the known high mobility of S atoms on heterogeneous HDS catalysts.[32] It has been reported that the presence of the promoter element increased the mobility of the surface S atoms, and the increase in HDS activity was correlated with this higher surface mobility. This behavior is consistent with the creation of vacancies or latent vacancies by the promoter atoms that allow the "walking" of the μ-sulfido bridges over the surface (cf. Scheme 4).

Conclusions

Multipoint coordination of thiolate S atoms in 3-fold "hollows" (i.e. μ_3-SR coordination) of a metal complex or, presumably, a catalyst surface drastically reduces the C−S bond dissociation energy. The BDE is lowered to the point that C−S bond homolysis of a coordinated aryl thiolate was observed at temperatures only slightly above room temperature (35 °C). Therefore it is unlikely that C−S bond dissociation is the rate determining step in actual HDS catalysis, usually practiced at much higher temperatures (≥350 °C).

The rate determining step on real catalysts appears to be related to the rate of creation of sulfur vacancies on the catalyst surface, i.e. the rate determining step is the removal of surface sulfur (as H_2S) that allows the substrate to adsorb on the catalyst surface, and it is this step that requires the high temperature in the catalytic reaction. Surprisingly, relatively little work has been done on the commercial catalysts that identifies the slow step of the HDS reaction. Moser et al., using a transient pulse reactor, showed that H_2S was the last product to evolve during a pulse of H_2.[26] Also, the most active HDS catalysts are those that have the lowest onset temperature for H_2S evolution during temperature-programmed reaction.[35] These results are consistent with the proposition that the rate of S removal determines the overall HDS activity of a heterogeneous catalyst. This conclusion was also reached on the basis of a consideration of bond energies,[36] and a theoretical treatment of small clusters also indicated that release of sulfur is important in determining the rate of reaction.[37]

A simple sequence of reactions, hydrogenation,[24b,c] E_2 elimination to form a surface bound thiolate, followed by C−S bond homolysis, presents a unified picture for HDS of thiols, thiophenes, and benzothiophenes that is consistent with the product slate, parallels the behavior of thiols, etc. on clean metal surfaces,[38] and is consistent with the relatively high oxidation state of the sulfided catalyst.

Experimental Section

General Considerations. All manipulations and reactions were conducted under a nitrogen atmosphere by use of standard Schlenk line techniques or by use of a glovebox. A stainless steel Parr High Pressure Reactor was used for all high-temperature and high-pressure reactions. All solvents were distilled and dried prior to use: toluene, tetrahydrofuran (THF), and diethyl ether from Na/benzophenone; dichloromethane, hexane, acetonitrile, and decahydronaphthalene (decalin) from CaH_2; and ethanol from Mg. $Cp'_2Mo_2Co_2S_3(CO)_4$ (**1**),[39] $Cp'_2Mo_2Co_2S_4(CO)_2$ (**2**),[40] cyclopropylmethanethiol,[41] and the thietanes[42] were prepared by published procedures. All other reagents were purchased from Aldrich Chemical Company, Lancaster, or Strem Chemical, Inc. ^{1}H-NMR data were collected on a Bruker AM-300 or Bruker WM-360 spectrometer. ^{1}H-NMR spectra were referenced to the solvent's residual proton resonance: C_6D_6 δ 7.15; $C_6D_5CD_3$ δ 2.09; CD_3CN δ 1.93; $(CD_3)_2CO$ δ 2.05. The program DNMR5 was obtained from the Quantum Chemistry Program Exchange, Indiana University, Bloomington, IN., Program No. 365, and was used to determine the simulated exchange broadened NMR spectra. FT-IR spectra were obtained on a Nicolet 5-DXB spectrometer and the spectra were corrected for background and solvent effects. GC-MS data were collected on a Finnigan spectrometer. Elemental analyses were done by the Microanalysis Laboratory, The University of Michigan.

(28) (a) Topsøe, H.; Clausen, B. S.; Topsøe, N.-Y.; Zeuthen, P. *Stud. Surf. Sci. Catal.* **1989**, *53*, 77. (b) Topsøe, H.; Clausen, B. S.; Topsøe, N.-Y.; Nørskov, J. K.; Ovesen, C. V.; Jacobsen, C. J. H. *Bull. Soc. Chim. Belg.* **1995**, *104*, 283.

(29) Startsev, A. N. *Catal. Rev.-Sci. Eng.* **1995**, *37*, 353.

(30) (a) Topsøe, H.; Clausen, B. S. *Appl. Catal.* **1986**, *25*, 273. (b) Burch, R.; Collins, A. *Appl. Catal.* **1985**, *17*, 273. (c) Kalthod, D. G.; Weller, S. W. *J. Catal.* **1986**, *98*, 572.

(31) Konuma, K.; Takase, S.; Kameda, N.; Itabashi, K. *J. Mol. Catal.* **1993**, *79*, 229.

(32) Massoth, F. E.; Zeuthen, P. *J. Catal.* **1994**, *145*, 216.

(33) Topsøe, H.; Clausen, B. S.; Candia, R.; Wivel, C.; Mørup, S. *J. Catal.* **1981**, *68*, 433.

(34) (a) Komatsu, T.; Hall, W. K. *J. Phys. Chem.* **1992**, *96*, 8131. (b) Sundberg, P.; Moyes, R. B.; Tomkinson, J. *Bull. Soc. Chim. Belg.* **1991**, *108*, 967.

(35) (a) Scheffer, B.; Dekker, N. J. J.; Mangnus, P. J.; Moulijn, J. A. *J. Catal.* **1990**, *121*, 31. (b) de Beer, V. H. J.; van der Aalst, M. J. M.; Machiels, C. J.; Schuit, G. C. A. *J. Catal.* **1976**, *43*, 78.

(36) Nørskov, J. K.; Clausen, B. S.; Topsøe, H. *Catal. Lett.* **1992**, *13*, 1.

(37) Neurock, M.; van Santen R. A. *J. Am. Chem. Soc.* **1994**, *116*, 4427.

(38) (a) Wiegand, B. C.; Uvdal, P.; Friend, C. M. *J. Phys. Chem.* **1992**, *96*, 4527. (b) Wiegand, B. C.; Napier, M. E.; Friend, C. M.; Uvdal, P. *J. Am. Chem. Soc.* **1996**, *118*, 2962.

(39) Curtis, M. D.; Williams, P. D.; Butler, W. M. *Inorg. Chem.* **1988**, *27*, 2853.

(40) Brunner, H.; Wachter, J. *J. Organomet. Chem.* **1982**, *240*, C41.

(41) Cossar, B. C.; Fournier, J. O.; Fields, D. L.; Reynolds, D. D. *J. Org. Chem.* **1962**, *27*, 93.

(42) (a) Dodson, R. M.; Jancis, E. H.; Klose, G. *J. Org. Chem.* **1970**, *35*, 2520. (b) Sander, M. *Chem. Rev.* **1966**, *66*, 341.

Table 3. NMR Spectra of **1**·$SC_6H_4Me^-$ at Various Temperatures

temp (K)	bound thiolate	CpH	$CpCH_3$
249	7.32 (m, 2H), 6.82 (m, 2H), 2.20 (s, 3 H)	5.70 (m, 1H), 5.51 (m, 2H), 5.31 (m, 1H), 5.22 (m, 1H), 5.18 (m, 1H), 5.01 (m, 1H), 4.86 (m, 1H)	2.01 (s, 3H), 1.99 (s, 3H)
263	7.32 (m, 2H), 6.82 (m, 2H), 2.20 (s, 3H)	5.70 (m, 1H), 5.51 (m, 2H), 5.31 (m, 1H), 5.23 (m, 1H), 5.19 (m, 1H), 5.03 (m, 1H), 4.88 (m, 1H)	2.01 (s, 3H), 2.00 (s, 3H)
273	7.32 (m, 2H), 6.82 (m, 2H), 2.20 (s, 3H)	5.70 (m, 1H), 5.51 (m, 2H), 5.31 (m, 1H), 5.26 (m, 1H), 5.21 (m, 1H), 5.03 (m, 1H), 4.89 (m, 1H)	2.02 (s, 6H)
283	7.32 (m, 2H), 6.82 (m, 2H), 2.20 (s, 3H)	5.70 (m, 1H), 5.51 (m, 2H), 5.31 (m, 1H), 5.26 (m, 1H), 5.21 (m, 1H), 5.04 (m, 1H), 4.91 (m, 1H)	2.03 (s, 6H)

Reaction of 1 with $[(C_6H_5CH_2)N(CH_3)_3][SC_6H_4CH_3]$ ($[BzNMe_3][SC_6H_4CH_3]$). A 25-mL Erlenmeyer flask was charged with cluster **1** (50 mg, 0.074 mmol) and $[BzNMe_3][SC_6H_5CH_3]$ (45 mg, 0.15 mmol). Acetonitrile (4 mL) was added and the solution was stirred for 1 h. The solution was filtered, then layered with diethyl ether to induce crystallization. Dark green crystals (compound **3b**) were obtained (32 mg). Anal. Calcd for $C_{33}H_{37}Co_2Mo_2NO_4S_4$: C, 41.70; H, 4.05; N, 1.52. Found: C, 42.51; H, 4.10; N, 1.46. IR (CH_3CN) υ(CO): 1962 and 1913 cm^{-1}. ^{1}H-NMR at 295 K (CD_3CN): bound thiolate, δ 7.34 (d, 2H), 6.82 (d, 2H), 2.22 (s, 3H); cation, δ 7.54 (m, 5H), 4.37 (s, 2H), 2.98 (s, 9H); CpH: δ 5.50 (m, 2H) plus three additional broad peaks between 4.9 and 6.0 ppm; $CpCH_3$, δ 2.04 (s, 6H). Additionally, ^{1}H-NMR spectra for compound **3b** were collected at 249, 263, 273, and 283 K. These spectra are summarized in Table 3.

Reaction of 1 with $(NEt_4)(SC_6H_4CH_3)$. A resealable NMR tube was charged with a solution of cluster **1** (17 mg, 0.025 mmol) in $(CD_3)_2$-CO (0.5 mL). A solution of $(NEt_4)(SC_6H_4CH_3)$ (13 mg, 0.051 mmol) in $(CD_3)_2CO$ (0.5 mL) was added to the frozen solution of cluster **1**. The tube was placed immediately into a cooled (213 K) NMR probe and a spectrum was recorded. Compound **4a** ^{1}H-NMR ($(CD_3)_2CO$, 213 K): bound thiolate, δ 7.30 (d, 2H), 6.72 (d, 2H), 2.10 (s, 3H); CpH, δ 5.29 (m, 2H), 5.21 (m, 2H), 5.07 (m, 2H), 4.92 (m, 2H); $CpCH_3$: δ 1.96 (s, 6H). At 266 K, resonances appeared in the proton NMR spectrum that corresponded to a compound analogous to that of compound **3b**. Compound **4b** ^{1}H-NMR ($(CD_3)_2CO$, 263K): bound thiolate, 7.39 (d, 2H), 6.68 (d, 2H), 2.19 (s, 3H); CpH, δ 5.72 (m, 1H), 5.48 (m, 2H), 5.34 (m, 1H), 5.28 (m, 1H), 5.24 (m, 1H), 4.97 (m, 1H), 4.89 (m, 1H); $CpCH_3$: δ 2.03 (s, 3H), 2.00 (s, 3H).

Thermal Decomposition of Compound 3b. A resealable NMR tube was charged with crystals of **3b** (15 mg) and CD_3CN (1 mL). An oil bath was heated to 80 °C, then the tube was placed in the oil bath. The progress of the reaction was monitored periodically by ^{1}H-NMR spectroscopy. After 1 h, all of compound **3b** had reacted. The solvent was removed *in vacuo* and analyzed by GC-MS spectroscopy; three organic products were detected (*m*/*e*): toluene-d_1 (93), $(C_6H_5$-$CH_2)N(CH_3)_2$ (135), and $CH_3SC_6H_4CH_3$ (138). A dark solid remained after the solvent was removed. The solid was identified as the monoanion of **2**. IR (CH_3CN): υ(CO) 1898 and 1865 cm^{-1}.

Reaction of 1 with ^{t}BuSNa. A resealable tube was charged with cluster **1** (20 mg, 0.30 mmol), ^{t}BuSNa(4.0 mg, 0.30 mmol), and CH_3-CN (1.0 mL). The solution was heated to 80 °C for 2.5 h. GC-MS analysis of the head gases revealed isobutane (*m*/*e* 58). No other organic products were detected. The monoanion of **2** was detected by IR analysis of the solution: υ(CO) 1898 and 1865 cm^{-1}.

Reaction of 1 with (*cyclo*-C_3H_5)CH_2SLi. A resealable NMR tube was charged with cluster **1** (20 mg, 0.07 mmol), (*cyclo*-C_3H_5)CH_2SLi (10 mg, 0.11 mmol), and CD_3CN (0.7 mL). The solution was heated to 80 °C. The progress of the reaction was monitored periodically by ^{1}H-NMR spectroscopy. After 4 h, the tube was cooled to room temperature. The head gases were analyzed by GC-MS. GC-MS (*m*/*e*): 1-butene-d_1 (57). The NMR solution was removed *in vacuo* and analyzed by GC-MS; no other organic products were detected. A dark solid remained after removal of the solvent. IR (CH_3CN): υ(CO) 1898 and 1865 cm^{-1}.

Reaction of $(NEt_4)(1{\cdot}SC_6H_4CH_3)$ (4b) with CF_3SO_3H. A resealable NMR tube was charged with cluster **1** (16 mg, 0.024 mmol), $(NEt_4)(SC_6H_4CH_3)$ (16 mg, 0.063 mmol), and CD_3CN (1.0 mL). A room temperature ^{1}H-NMR spectrum revealed the thiolate complex **4b**—analogous to compound **3b**—was formed. The tube was then placed in an ethanol/N_2 slush bath (T = <−100 °C). Triflic acid (approximately 10 μL) was added to the frozen solution. The tube was then placed immediately into a precooled (213 K) NMR probe and a proton spectrum was recorded. ^{1}H-NMR (CD_3CN, 213 K): cluster **1**, δ 5.83 (m, 4H), 5.49 (m, 4H), 2.13 (s, 6H); $CH_3C_6H_4SH$, δ 7.40 (d, 2H), 7.20 (d, 2H), 2.33 (s, 3H). These products were identified based on comparison with NMR spectra taken of authentic samples. The proton resonance for the thiol group in compound $CH_3C_6H_4SH$ was not observed in either the experimental or authentic sample.

Reaction of $[NEt_4][1{\cdot}SC(CH_3)_3]$ (5) with $CF_3SO_3CH_3$. A 25-mL Schlenk flask was charged with cluster **1** (21 mg, 0.031 mmol), (NEt_4)(S-^{t}Bu) (29 mg, 0.11 mmol), and $(CD_3)_2CO$ (1 mL). The mixture was stirred for 1 h, then transferred to a resealable NMR tube. The tube was placed in an ethanol/N_2 slush bath (T = <−100 °C). CF_3-SO_3CH_3 (ca. 20 μL) was added to the frozen solution. The tube was then placed immediately into a precooled (243 K) NMR probe and a spectrum was recorded. ^{1}H-NMR ($(CD_3)_2CO$, 243 K) compound **5a**: bound thiolate, δ 1.39 (s, 9H); bound CH_3^+, δ 2.38 (s, 3H); CpH, δ 5.82 (m, 1H), 5.66 (m, 1H), 5.62 (m, 1H), 5.58 (m, 1H), 5.28 (m, 1H), 5.22 (m, 1H), 5.13 (m, 2H); $CpCH_3$: δ 2.11 (s, 3H), 2.08 (s, 3H); $CH_3SC(CH_3)_3$, δ 1.98 (s, 3H), 1.22 (s, 9H); cluster **1**, δ 5.84 (m, 2H), 5.51 (m, 2H), 2.14 (s, 6H). Spectra were also recorded at 263, 283, and 295 K. The intensity of the peaks associated with compound **5a** decreased as a function of temperature, while the intensity of the peaks characteristic of cluster **1** increased.

Reaction of $[NEt_4][1{\bullet}SC(CH_3)_3]$ with CH_3I. A 50-mL Schlenk flask was charged with cluster **1** (59 mg, 0.074 mmol), $[NEt_4][SC$-$(CH_3)_3]$ (68 mg, 0.31 mmol), and THF (6 mL). After 5 min of stirring, an aliquot of the reaction mixture was removed via syringe and injected into a liquid IR cell. IR (THF) 1953 and 1898 cm^{-1}. CH_3I (≈30 μL) was added to the reaction mixture. A white precipitate ($[NEt_4][I]$) developed immediately. An aliquot of the reaction mixture was removed for analysis by IR spectroscopy. IR (THF) of cluster **1**: 2009, 1988, and 1955 cm^{-1}. The identical result was obtained when $[NEt_4]$-$[1{\cdot}SC(CH_3)_3]$ was allowed to react with $(CH_3)_3CI$. Cluster **1** was recovered in a 75% yield. The organic product, $((CH_3)_3C)_2S$, was detected by a GC-MS analysis of the reaction solution (*m*/*e* 146).

Reaction of 1 with (*cyclo*-C_3H_5)CH_2SH. A resealable NMR tube was charged with cluster **1** (22 mg, 0.033 mmol), (*cyclo*-C_3H_5)CH_2SH (4 mL, 0.045 mmol), and toluene-d_8 (1 mL). The solution was heated to reflux and the progress of the reaction was monitored periodically by ^{1}H-NMR spectroscopy. After approximately 4 h, the reaction was complete. The cluster **2** was identified by comparison of the NMR spectrum with those of authentic samples. The only organic product that formed was 1-butene: ^{1}H-NMR ($C_6D_5CD_3$) of 1-butene: δ 0.85 (t, 3H), 1.91 (m, 2H), 4.96 (m, 1H), 5.01 (m, 1H), 5.77 (m, 1H). GC-MS of NMR solution (*m*/*e*): 1-butene (56).

Kinetic Measurements of Thiol Desulfurization Reactions Mediated by 1. Thiol kinetic experiments were conducted under pseudo-first-order conditions with the concentration of the thiol in 10-fold excess or more. Kinetic data for the desulfurization of aromatic and aliphatic thiols were obtained by monitoring the disappearance of the CO stretching band centered at 1959 cm^{-1} of cluster **1** (Figure 1). The desulfurization reactions were performed in a 50-mL Schlenk flask equipped with a reflux condenser. An oil bubbler was attached to the reflux condenser. The flask was placed in an insulated oil bath and constant temperature was maintained using a RFL model 76K-1 temperature controller. In a typical experiment, 5.0 mL of a 2×10^{-3} M solution of cluster **1** in decalin was syringed into the preheated reaction flask followed by addition of 5.0 mL of thiol stock solution. After 30 s, a syringe was used to remove an aliquot of the reaction

mixture. The aliquot was injected into an evacuated vial, then cooled immediately in an ice bath to ensure no further reaction occurred. The solution was then transferred to a liquid IR cell for analysis. Plots of $\ln(A_t)$ (A_t is the absorbance of the 1959 cm^{-1} band) versus time were linear over several half-lives ($r^2 > 0.991$) for all reactions. The slopes of these lines yielded observed rate constants (k_{obs}). The observed rate constants were then used to derive the second-order rate constants (Table 1, Supporting Information). Activation parameters for the desulfurization of the various thiols are listed in Table 2.

Effect of Thiol Concentration on the Rate of Desulfurization. A 0.12 M stock solution of C_6H_5SH in decalin was prepared. This stock solution was used to prepare 0.068 and 0.031 M solutions. A 0.17 M stock solution of $CH_3OC_6H_4SH$ in decalin was prepared. This stock solution was used to prepare a 0.085 M solution. The various C_6H_5SH and $CH_3OC_6H_4SH$ solutions were used to determine the effect of thiol concentration on the rate of the desulfurization reaction. The rate constants are listed in Table 4, Supporting Information.

Effect of CO on the Rate of Desulfurization. A 0.12 M stock solution of C_6H_5SH in decalin was prepared. A 50-mL Schlenk flask equipped with a reflux condenser was heated to 125 °C, then charged with the thiol stock solution (5 mL) and an equal volume of a 2×10^{-3} M solution of cluster **1**. Both solutions were thoroughly degassed with CO prior to injection into the Schlenk flask. The desulfurization reaction was performed under a slow purge of CO gas at 1 atm. The rate constant for this reaction was determined to be $k = 0.86(6) \times 10^{-3}$ M^{-1} s^{-1}.

Acknowledgment. The authors are grateful to the National Science Foundation for support of this research (Grant Nos. CHE-9205018 and CHE-9523056).

Supporting Information Available: Tables of second order rate constants for the desulfuization of thiols by cluster **1** and k_{obs} as a function of thiol concentration (1 page). See any current masthead page for ordering and Internet access instructions.

JA9621096